Portable Chest-Worn Device for Simultaneous Detection of Phonocardiogram and Seismocardiogram Using Piezoelectric Films Sensors

Pamela Salas Canales(✉), José Mejía Muñoz, and Rafael Gonzalez-Landaeta

BIOCIM Research Group, Universidad Autónoma de Ciudad Juárez, Ciudad Juárez, Chihuahua 32310, México
al228162@alumnos.uacj.mx

Abstract. The simultaneous detection of different heart signals provides information about cardiovascular health but typically involves attaching multiple sensors to the body, which can lead to discomfort during long-term measurements. In this work, we propose a different approach to simultaneously detect the phonocardiogram (PCG) and seismocardiogram (SCG). It relies on using two piezoelectric films implemented in a single portable chest-worn device, reducing the number of devices attached to the body. Besides, since these sensors do not require any power supply, the power consumption is considerably reduced. This innovative approach offers a potentially more comfortable alternative for long-term applications, reducing user discomfort. Because both signals have different frequency components, both sensors were strategically coupled to a stethoscope membrane using a custom-built case. The device was tested on a healthy volunteer. It was able to simultaneously detect the PCG with an SNR higher than 34 dB and the SCG with an SNR higher than 62 dB. The electronic circuitry was battery-supplied, and its current consumption was lower than 65 uA. The possibility of establishing a client/server connection via sockets was also demonstrated, which allows sending of data to the cloud/fog where intelligence algorithms could be implemented.

Keywords: Chest-worn device · Phonocardiogram · Seismocardiogram

1 Introduction

The genesis of the phonocardiogram (PCG) and the seismocardiogram (SCG) comes from the precordial vibrations, which have infrasound and audible components [1]. Regarding the PCG, this signal can offer insights into both the cardiac valve dynamics and arterial blood pressure (ABP) by examining different aspects of the waveform [2, 3]. The recording of heart sounds is commonly done by using microphones of different technologies [4]. However, alternatives based on accelerometers [5], Lead Zirconate Titanate (PZT) [6], and Polyvinylidene Difluoride (PVDF) piezoelectric sensors [7] have also been proposed. On the other hand, the SCG is the recording of the vibrations of the

J. de J. A. Flores Cuautle et al. (Eds.): CNIB 2023, IFMBE Proceedings 96, pp. 313–320, 2024.
https://doi.org/10.1007/978-3-031-46933-6_33

body produced by the heartbeat [8] and provides information on the mechanical activity of the heart. SCG can be detected by piezoelectric accelerometers, MEMS accelerometers, triaxial gyroscopes, and laser vibrometers [9]. Systems based on accelerometers, gyroscopes, and microphones must deal with noise problems and high current consumption since they have embedded preprocessing stages, including amplifiers and resistors. Even so, the small size of current microphones and accelerometers makes them ideal for implementation in wearable systems with a low form factor, which results in a more comfortable system for long-term measurements.

The simultaneous detection of cardiac signals helps to estimate other physiological parameters [10]. Assessing the temporal relationship between a proximal signal and a distal signal makes it possible to estimate the systolic blood pressure (SBP) without using a cuff. The pulse arrival time (PAT), pulse transit time (PTT), and pulse wave velocity (PWV) [11] are commonly analyzed using electrocardiogram (ECG), photoplethysmogram (PPG) [12, 13], seismocardiogram (SCG) [14], ballistocardiogram (BCG) [15] and phonocardiogram [16] signals and have been used to develop portable devices for cuffless and continuous detection of ABP. The problem with these approaches is that some systems require many sensors attached to the body, which causes discomfort to the subject in long-term monitoring. To tackle this, some devices have been proposed that use the correlation between the PTT and the systolic blood pressure for continuous ABP measurement using a minimum number of sensors. Devices that detect ECG and PPG signals at the bicep and ear or only at the bicep [17], a watch-based device that measures single-lead ECG, tri-axial SCG, and multi-wavelength PPG [18], and a single chest-worn device the measures the PPT using SCG, and PPG [19], have been proposed.

This work proposes a new approach to simultaneously detect PCG and SCG signals from a single point on the thorax. A similar proposal has been presented in [20], using a single CM-01B contact microphone to simultaneously detect respiration, SCG, and heart sounds. Each signal was extracted from the raw data by filtering, which can lead to signal distortion. The CM-01B sensor has an embedded field effect transistor (FET), a source of noise that degrades the Signal-to-Noise Ratio (SNR) of the signals and consumes 100 μA. Since the signal must be amplified, the total consumption of this system increases, which reduces the system's autonomy. A more sophisticated sensor based on an encapsulated accelerometer contact microphone that uses nano-gap transducers has also been proposed for detecting cardiopulmonary signals [5]. However, this sensor requires a high-precision fabrication technique. In this work, two commercials shielded PVDF (Polyvinylidene fluoride) piezoelectric film sensors are used, which do not require a power supply and reduce the contribution of electromagnetic interference. The two piezoelectric film sensors are attached to a stethoscope membrane using a custom-built case for portability. To the best of our knowledge, using these kinds of sensors to simultaneously detect the PCG and the SCG is a novelty approach that has yet to be proposed. So, the goal of this work is twofold: a new approach for sensing the infrasound and audible precordial vibrations, and to design a low-power electronic circuit for PCG and SCG detection with high SNR to simplify (in the future) the signal processing algorithms for estimating others cardiovascular parameters. The findings from this study serve as the foundation for creating a portable system that uses the temporal correlation between PCG and SCG signals to estimate the SBP at a single point on the chest.

2 Materials and Methods

2.1 Sensor Coupling

Two sensors were used to simultaneously detect PCG and SCG at a single point on the thorax: one was exclusively for PCG, while the other was for SCG. For each signal, the sensor used was the piezoelectric film sensor SDT1-028K from TE Connectivity, which has a capacitance of 2.78 nF, a minimum electrical impedance of 1 MΩ, and a maximum of 10 MΩ. When it is not attached to any surface, its resonance frequency is up to 10 MHz [21], and the frequency response can be limited by the low-pass response of the signal conditioning stages [7]. In this scenario, the frequency response can be adjusted to detect the frequency components of the S1 and S2 sounds of the PCG, which are in a bandwidth of 100 to 200 Hz and 50 to 250 Hz, respectively. If the sensor is attached to a surface, the bandwidth of the system is limited because the surface acts as a mechanical low-pass filter. Even so, the frequency response is still sufficient to detect the SCG [7], whose bandwidth ranges from 0 to 25 Hz. Both sensors were coupled to a Littmann® stethoscope membrane using a custom-built case (Fig. 1a), which allows the PCG sensor to be placed without direct contact with the membrane and the SCG sensor to be in direct contact with the stethoscope membrane. The case was designed in SolidWorks and 3D printed with resin. The coupling of the sensors to the stethoscope membrane is shown in Fig. 1b.

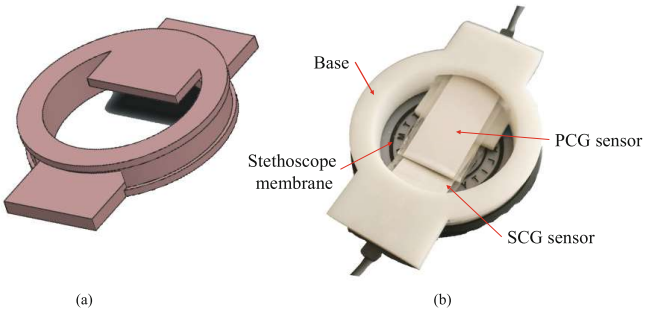

Fig. 1. Sensor coupling: (a) SolidWorks design, (b) 3D printed prototype.

2.2 Signal Acquisition

The circuits for the simultaneous detection of PCG and SCG signals consist of a charge amplifier that transforms charge variations from the sensor to an output voltage, an amplifier that adjusts the signal amplitude and the cutoff frequency, and a DC servo loop circuit to null DC components at the output.

The PCG detection circuit (Fig. 2a) was designed to work in a frequency range of 34 to 600 Hz, with a total gain of 55 dB, to observe as many frequency components of the S1 and S2 sounds as possible. The low-pass frequency response of the system was limited by the gain-bandwidth product of the amplifier (OA2) at a gain of 40 dB. The

high-pass response was limited by the charge amplifier (OA1), which has a sensitivity of 2.12 mV/pC. The SCG detection circuit (Fig. 2b) works in a frequency range of 3.3 Hz to 34 Hz with a total gain of 35 dB. The low-pass frequency response of the system was limited by $R_Y C_4$, while the high-pass response was limited by the charge amplifier (OA4), which has a sensitivity of 2.12 mV/pC. Both detection circuits were implemented using the operational amplifier TLV2322 from Texas Instruments and were supplied by a single 3.7 V/1000 mAh Lithium-Ion battery.

The auscultation point selected was the pulmonary valve located in the second intercostal space to the left of the sternum. This auscultation point was chosen because, in previous tests, it was the point where a greater amplitude of both signals was obtained. The ECG (lead II) was also detected using the AD8232 Single Lead Heart Rate Monitor (Analog Devices). The signals were simultaneously acquired at 1 kSa/s using a National Instruments USB 6341 data acquisition system controlled by an algorithm developed in LabVIEW. The signals acquisition was performed following the CEI-2023–1-853 measurement protocol approved by the UACJ ethics committee. The protocol consisted of detecting the PCG, SCG, and ECG signals from a healthy adult volunteer who remained seated during the process (Fig. 2c) and gave his/her informed consent to participate in the procedure.

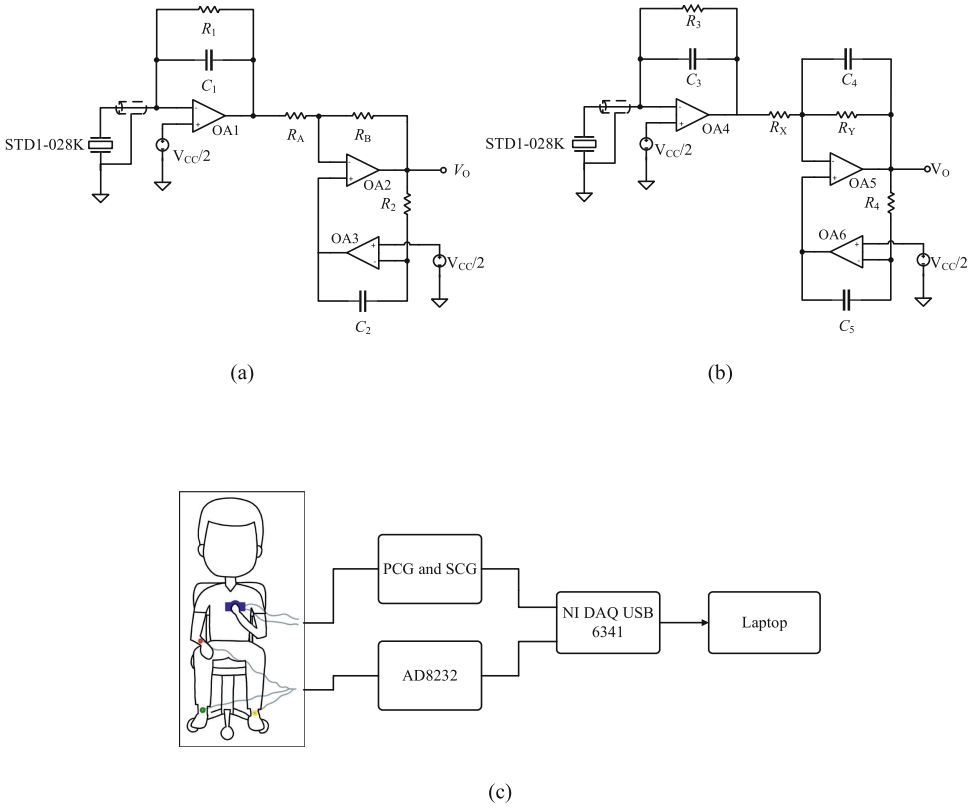

Fig. 2. (a) Designed circuit for PCG detection, (b) designed circuit for SCG detection, (c) Setup for detecting the PCG, SCG, and ECG simultaneously.

A server/client link via TCP/IP sockets connection was implemented to demonstrate the ability of the device to send the acquired signals to the cloud/fog. For this, the signals were acquired using the ESP32 microcontroller, and via TCP/IP sockets connection, the corresponding data to each signal was sent and saved in a local computer, as shown in Fig. 3.

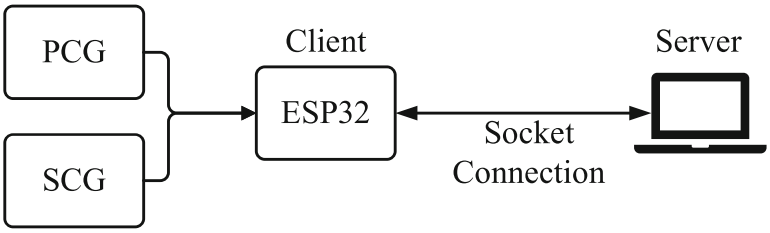

Fig. 3. Client/server connection.

3 Results

The voltage noise spectral density of the circuits of Fig. 2a and 2b are depicted in Fig. 4a and Fig. 4b, respectively. The output noise root mean square (RMS) voltage of the PCG circuit is about 1.4 mV, and of the SCG circuit is about 50 μV. The current consumption of both circuits working together was lower than 65 μA (240 μW). With these characteristics, the system was able to detect the signals with an SNR higher than 34 dB for the PCG and higher than 62 dB for the SCG.

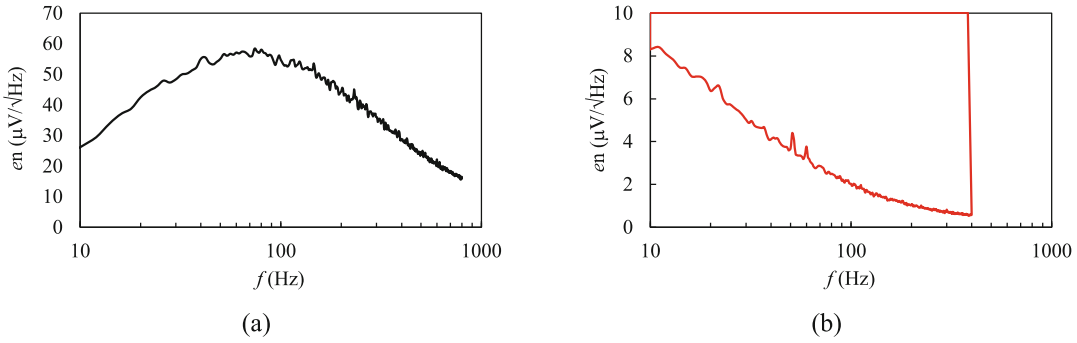

Fig. 4. Voltage noise spectral density of the circuit used for detecting the PCG (a) and the SCG (b).

Figure 5 shows the PCG and the SCG simultaneously detected and compared with the Lead II ECG as a reference. The S1 and S2 of the PCG were detected by the sensor that was not attached to the surface of the membrane. The sensor attached to the surface of the membrane detected the infrasound chest vibrations that give rise to SCG. When measuring with the SCG sensor, the motion artifacts can have a significant impact, which can cause signal distortion; this is because the sensor is located near the chest wall. To get

accurate results, it is crucial to ensure that the subject stays still during the measurement process. By analyzing the PCG and SCG signals displayed in Fig. 5, it becomes feasible to estimate the time correlation between S1 and S2 of the PCG and the main waves of the SCG, which could be an alternative method for estimating SBP using a single chest-worn device.

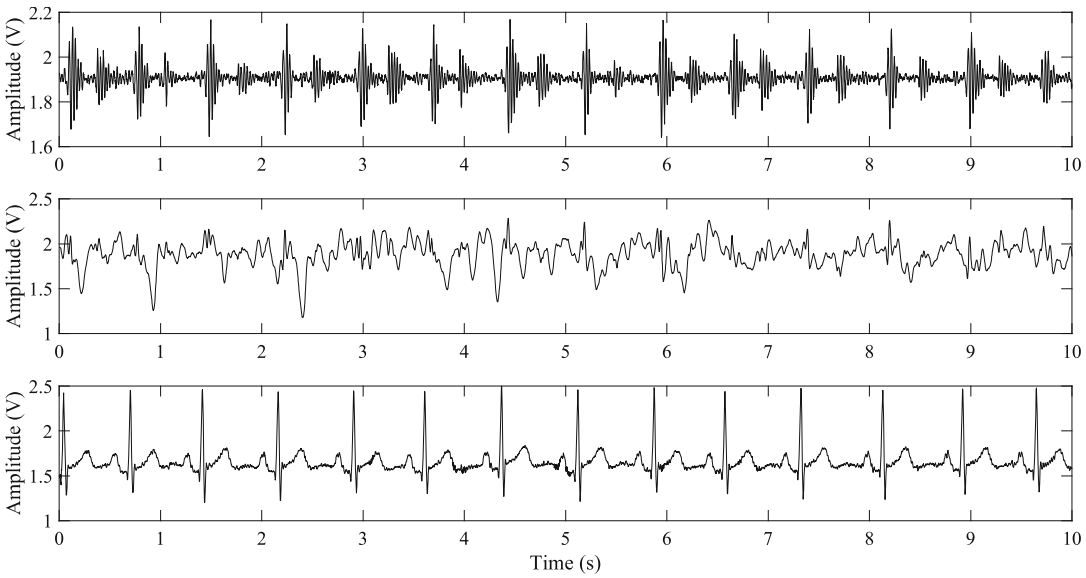

Fig. 5. Raw signals of the PCG (upper trace) and SCG (middle trace) detected with circuits shown in Fig. 2. ECG (bottom trace) detected with the AD8232. All signals are from the same subject and were acquired simultaneously.

Figure 6 shows the PCG and SCG signals acquired with the ESP32 microcontroller and sent via socket connection to a local computer. This demonstrates the possibility of sending information to the cloud/fog without degrading the signal quality. With this approach, artificial intelligence algorithms could extract signal features using fewer hardware resources, which reduces power consumption significantly.

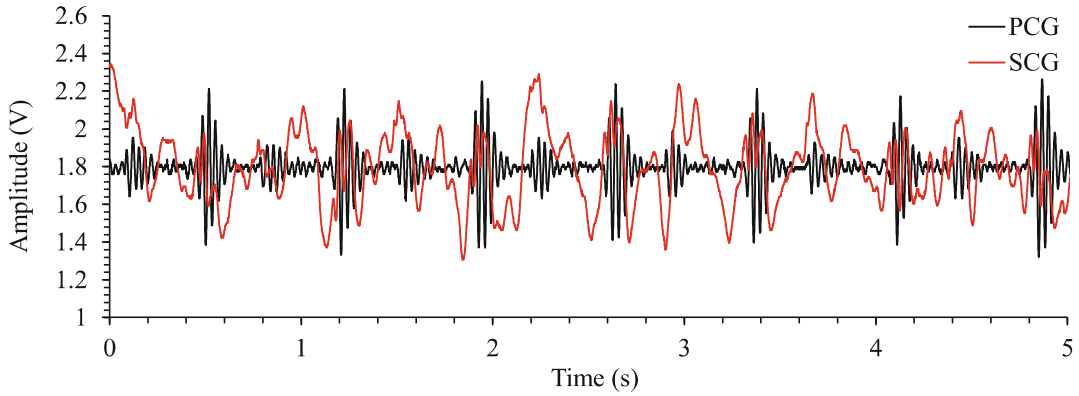

Fig. 6. FCG and SCG signals acquired using the microcontroller and sockets connection.

4 Conclusions

A different approach has been proposed to simultaneously detect the PCG and SCG, which was implemented in a portable and low-power chest-worn device. It relies on using two commercial piezoelectric films, reducing the number of devices attached to the body and the power consumption. The electronic circuitry was battery-supplied, and the total current consumption was lower than 65 uA, making it feasible for long-term measurements. Regarding the PCG, the SNR was higher than 34 dB, making it possible to detect the S1 and S2. For the SCG, the SNR was higher than 62 dB, allowing it to detect the main waves of the signal. The quality of the detected signals simplifies the processing algorithms to detect signal features, which helps estimate, for example, systolic blood pressure. The feasibility of using piezoelectric sensors to detect both signals was demonstrated. However, it must be considered that the coupling of each sensor on the thorax plays an important role due to the different frequency components of each signal. Using piezoelectric sensors helps reduce the power consumption that usually goes to sensors such as microphones and accelerometers. However, it should be noted that these sensors are more prone to movement artifacts. The results obtained in this study are the starting point for developing a portable system that makes it possible to estimate systolic blood pressure by taking measurements at a single point on the thorax.

References

1. Di Rienzo, M., et al.: Wearable seismocardiography: towards a beat-by-beat assessment of cardiac mechanics in ambulant subjects. Auton. Neurosci. **178**, 50–59 (2013)
2. Lim, K.H., et al.: Correlation of blood pressure and the ratio of S1 to S2 as measured by esophageal stethoscope and wireless bluetooth transmission. Pak. J. Med. Sci. **24**(9), 1023–1027 (2013)
3. Omari, T., Bereksi-Reguig, F.: A new approach for blood pressure estimation based on phonocardiogram. Biomed. Eng. Lett. **9**, 395–406 (2019)
4. Shyam Kumar, P., Ramasamy, M., Varadan, V.K.: Evaluation of signal quality from a wearable phonocardiogram (PCG) device and personalized calibration. Electronics **11**(17), 2655 (2022)
5. Gupta, P., Moghimi, M.J., Jeong, Y., Gupta, D., Inan, O.T., Ayazi, F.: Precision wearable accelerometer contact microphones for longitudinal monitoring of mechano-acoustic cardiopulmonary signals. NPJ Digit. Med. **3**(1), 19 (2020)
6. Chen, Z., Chen, D., Xue, L., Chen, L.: A piezoelectric heart sound sensor for wearable healthcare monitoring devices. In: Mucchi, L., Hämäläinen, M., Jayousi, S., Morosi, S. (eds.) BODYNETS 2019. LNICSSITE, vol. 297, pp. 12–23. Springer, Cham (2019). https://doi.org/10.1007/978-3-030-34833-5_2
7. Vazquez, K., Cota, J., Sifuentes, E., Gonzalez, R.: High signal-to-noise ratio phonocardiogram using a shielded PVDF film sensor. IEEE Lat. Am. Trans. **14**(3), 1139–1145 (2016)
8. Castiglioni, P., Faini, A., Parati, G., Di Rienzo, M.: Wearable seismocardiography. In: 29th Annual International Conference of the IEEE Engineering in Medicine and Biology Society, pp. 3954–3957. IEEE (2007)
9. Taebi, A., Solar, B., Bomar, A., Sandler, R., Mansy, H.: Recent advances in seismocardiography. Vibration **2**(1), 64–86 (2019)
10. Soliman, M.M., Ganti, V.G., Inan, O.T.: Toward wearable estimation of tidal volume via electrocardiogram and seismocardiogram signals. IEEE Sens. J. **22**(18), 18093–18103 (2022)

11. Tabei, F., Gresham, J.M., Askarian, B., Jung, K., Chong, J.W.: Cuff-less blood pressure monitoring system using smartphones. IEEE Access **8**, 11534–11545 (2020)
12. Tjahjadi, H., Ramli, K.: Review of photoplethysmography based non-invasive continuous blood pressure methods. In: 2017 15th International Conference on Quality in Research (QiR): International Symposium on Electrical and Computer Engineering, pp. 173–178. IEEE, Nusa Dua, Bali, Indonesia (2017)
13. Vajanarat, T., Lek-uthai, A.: A comparison of cuff-less blood pressure estimation between pulse arrival time and pulse transit time using photoplethysmography. In: 2020 17th International Conference on Electrical Engineering/Electronics, Computer, Telecommunications and Information Technology (ECTI-CON), pp. 13–16. IEEE, Phuket, Thailand (2020)
14. Imtiaz, M.S., et al.: Correlation between seismocardiogram and systolic blood pressure. In: 2013 26th IEEE Canadian Conference on Electrical and Computer Engineering (CCECE), pp. 1–4. IEEE, Regina, SK, Canada (2013)
15. Kim, C.-S., Carek, A.M., Mukkamala, R., Inan, O.T., Hahn, J.-O.: Ballistocardiogram as proximal timing reference for pulse transit time measurement: potential for cuffless blood pressure monitoring. IEEE Trans. Biomed. Eng. **62**(11), 2657–2664 (2015)
16. Gonzalez-Landaeta, R., Ramirez, B., Mejia, J.: Estimation of systolic blood pressure by random forest using heart sounds and a ballistocardiogram. Sci. Rep. **12**, 17196 (2022)
17. Griggs, D., et al.: Design and development of continuous cuff-less blood pressure monitoring devices. In: 2016 IEEE SENSORS, pp.1–3. IEEE, Orlando, FL, USA (2016)
18. Ganti, V.G., Carek, A.M., Nevius, B.N., Heller, J.A., Etemadi, M., Inan, O.T.: Wearable cuff-less blood pressure estimation at home via pulse transit time. IEEE J. Biomed. Health Inform. **25**(6), 1926–1937 (2021)
19. Park, J., et al.: Cuffless and continuous blood pressure monitoring using a single chest-worn device. IEEE Access **7**, 135231–135246 (2019)
20. Bifulco, P., et al.: Monitoring of respiration, seismocardiogram and heart sounds by a PVDF piezo film sensor. Measurement **11**, 786–789 (2014)
21. TE Connectivity SDT Shielded Piezo Sensors. https://www.te.com/commerce/DocumentDelivery/DDEController?Action=showdoc&DocId=Data+Sheet%7FSDT_Shielded_Piezo_Sensors%7FA1%7Fpdf%7FEnglish%7FENG_DS_SDT_Shielded_Piezo_Sensors_A1.pdf%7FCAT-PFS0010. Accessed 10 July 2023